Hindawi Publishing Corporation
International Journal of Polymer Science
Volume 2013, Article ID 307525, 7 pages
http://dx.doi.org/10.1155/2013/307525

Research Article

Synthesis, Electrical Conductivity, and Dielectric Behavior of Polyaniline/V_2O_5 Composites

Shama Islam,[1] G. B. V. S. Lakshmi,[2] Azher M. Siddiqui,[1] M. Husain,[1] and M. Zulfequar[1]

[1] *Department of Physics, Jamia Millia Islamia, New Delhi 110025, India*
[2] *Material Science Group, Inter University Accelerator Centre, New Delhi 110025, India*

Correspondence should be addressed to M. Zulfequar; mzulfe@rediffmail.com

Received 31 March 2013; Accepted 12 June 2013

Academic Editor: Enrique Vigueras-Santiago

Conducting polymer composites of polyaniline/vanadium pentaoxide PANI/V_2O_5 (with different initial weight percentage of V_2O_5) has been synthesized by *in situ* polymerization method. DC conductivity of compressed pellets has been analyzed in the temperature range 300–550 K and was found to increase with V_2O_5 doping. This increase in conductivity is mainly due to band conduction. It has also been observed that the dielectric constant and dielectric loss increase with the level of doping of V_2O_5 but remain independent of the frequency (50 KHz–1 MHz). X-ray diffraction pattern shows some order of crystallinity of composites due to interaction of polyaniline with V_2O_5. UV-visible spectroscopy shows an increase in the optical band gap with doping.

1. Introduction

The conducting polymers have emerged as a new class of materials because of their unique electrical, optical, and chemical properties. By proper doping the conductivity of these materials can be varied from semiconducting to metallic regime, which offers new concept of charge transport mechanism. Among different conducting polymers, conductive polyaniline (PANI) has been studied extensively because of its ease of synthesis in aqueous media, its environmental stability, special electrical, and other properties. PANI and its derivatives have received much attention because of their various technological applications, reversible proton doping, high electrical conductivity, and ease of bulk synthesis. PANI is also a suitable candidate for a variety of technological applications such as solar cells, electromagnetic shielding, electrodes for rechargeable batteries, and sensors [1–11].

Many authors have studied the progress of chemical polymerization and doping of aniline and its derivatives. The effort was to correlate mechanisms of oxidation of anilines and properties of PANI such as electrical conductivity, molecular weight, and crystallinity. However, when they were taken in the composite form, their electrical as well as dielectric properties alter from those of basic materials. A number of groups had reported on the electrical conductivity and dielectric properties of composites of a variety of conducting polymers [12–15]. Recently heterogeneous conducting polymer composites, especially organic-inorganic composites, became the subject of extensive study. Among the base materials used, polyaniline (PANI) is one of the most extensively studied conducting polymer. Ever since its discovery in a pioneering work by Mc Diarmid et al. [16–21]. The DC conductivity of a conjugated polymer depends on the doping level, and for a given dopant in a particular polymer, the conductivity increases up to a certain level and then saturates.

The vanadium oxygen system (V_2O_5 and VO_2) has been widely studied because the system shows metal semiconductor transitions, which imply an abrupt change in their optical and electrical properties. For example, VO_2 exhibits a change in electrical resistivity in the order of 10^5 Ω cm over a temperature change of 0.1 at 68°C in a single crystal. This oxide is therefore used in thermal sensing and switching. Similarly, V_2O_5 has been a subject of several theoretical and applied studies, due to its industrial importance for many technological applications, such as heterogeneous catalyst. V_2O_5 also plays the role of active electrode in a rechargeable lithium battery. High electrochemical activity, high stability, and ease of thin film formation by numerous deposition

techniques led to its use as a highly promising intercalation material in solid state microbattery applications. It is the most stable oxide in the V–O system with an energy gap of ~2.2 eV and shows a semiconductor-metal transition at about 250°C [22–26].

In the present study, composites of PANI/V_2O_5 have been synthesized by *in situ* polymerization of aniline using ammonium persulphate ($(NH_4)\ S_2O_8$) as oxidizing agent, in the presence of V_2O_5. The V_2O_5 concentrations were varied from 0 to 40% weight. The composites obtained have different concentrations of V_2O_5.

In present work electrical conductivity by two-probe method and dielectric behavior by LCR methods of these synthesized composites have been studied. X-ray diffraction (XRD) and UV-visible absorption spectroscopy have been carried out to characterize these samples.

2. Experimental

All chemicals used were of analytical reagent (AR) grade. The monomer aniline was doubly distilled prior to use. Ammonium persulphate ($(NH_4)\ S_2O_8$), hydrochloric acid (HCl), and vanadium pentoxide V_2O_5 were used as received in the present study.

Polyaniline has been synthesized by *in situ* oxidative polymerization of aniline, hydrochloric acid (HCl), and ammonium persulphate ($(NH_4)\ S_2O_8$) as oxidant. The oxidant monomer ratio is 1 : 1.25. Aniline (1.25 M) has been dissolved in 10 mL of HCl (1 M) taken in 200 mL round bottom flask and stirred well. Further finely ground V_2O_5 powder taken in different (20, 30, and 40) wt% with respect to aniline concentration has been added to the previous mixture under vigorous stirring in order to keep V_2O_5 powder suspended in solution. The reaction mixture has been cooled up to 5°C, and the precooled solution of ammonium persulfate (1 M) has been slowly added drop by drop over a period of 30 min. The reaction has been allowed to proceed for 6–8 h. The mixture was further cooled down to 4°C for 24–36 hours. It was then filtered and washed with ammonia until filtrate was colorless. The dark colored polymer powder so obtained was dried thoroughly in an oven at 100°C until constant weight was attained, then grinded and sieved. PANI has been synthesized in the same manner in the absence of V_2O_5.

The DC conductivity of pure PANI and PANI/V_2O_5 composites was measured by using two-probe method in the temperature range 300–550 K. The powder was made into pellets of 1 cm diameter and different thickness for PANI/V_2O_5 composites. The bulk DC conductivity was measured by mounting between two steel electrodes inside a specially designed metallic sample holder [22]. The temperature was measured with a calibrated copper-constantan thermocouple mounted near the electrodes. The samples were annealed at a temperature of 100°C to avoid any effect of moisture absorption. These measurements were made at a pressure of about 10^{-3} Torr. A stabilized voltage of 1.5 V was applied across the sample, and the resultant current was measured with a picoammeter.

In order to get information about the crystallinity, X-ray diffraction patterns of all samples are recorded at room temperature by using a Panalytical (PW 3710) X-ray powder diffractometer with Cu Kα radiation. All the samples were scanned in angular range of 0–90° with scan speed of 0.01°/s under the similar conditions. UV-visible spectroscopy has been carried out using Camspec M550 double beam UV-visible spectrophotometer [22–26].

3. Results and Discussion

3.1. Temperature DC Conductivity Studies. The variation of DC conductivity with temperature for pure PANI and the PANI/V_2O_5 composites (with different wt%) is shown in Figure 1. Arrhenius plot of DC conductivity shows straight line behavior. The DC conductivity of pure PANI increased exponentially with doping, exhibiting semiconductor characteristics. The conductivity as a function of temperature can be represented by the relation [27]

$$\sigma_{DC} = \sigma_0 \exp\left(-\frac{\Delta E}{kT}\right), \quad (1)$$

where (ΔE) is the activation energy for the DC conduction mechanism, "k" is the Boltzmann constant, and "σ_0" is the preexponential factor. The activation energy (ΔE) has been calculated from the slope of Figure 1 for pure PANI and the PANI/V_2O_5. The DC conductivity of undoped PANI is measured to be 3.58×10^{-9} S/cm. After doping with different weight % of V_2O_5 the conductivity was found to change from 10^{-7} to 10^{-9} S/cm, attaining a maximum value at 30 weight % of V_2O_5 and then reduced at 40 weight % of V_2O_5. The doping of conducting polymers implies charge transfer, the associated insertion of a counter ion, and the simultaneous control of Fermi level or chemical potential. Through doping, electronic and optical properties of conducting polymers can be controlled over a long range. The electrical conductivity of conducting polymers results from mobile charge carriers introduced into the π-electronic system through doping. At low doping levels these charge carriers are self-localized and form nonlinear configurations. Because of large interchain transfer integrals, the transport of charge is believed to be principally along the conjugated chains, with interchain hopping as a necessary secondary condition [28–31]. When the polymer is heavily doped (40 weight %), the wave functions are delocalized over many lattice constants along the polymer chain. In PANI, since there are nearly degenerate ground states, the dominating charge carriers are polarons and bipolarons [32]. When PANI is doped with V_2O_5 hydrochloric acid, the charge carriers form nonlinear configurations, and as a result the conductivity does not change substantially. The nonlinear formation may be more in the case of heavy doping of 40 weight % of V_2O_5, due to which it exhibits lesser conductivity than 30 weight % doped polymer.

The activation energy ΔE, DC conductivity σ_{DC}, and preexponential factor σ_0 of pure PANI and PANI/V_2O_5 composites have been measured and tabulated in Table 1.

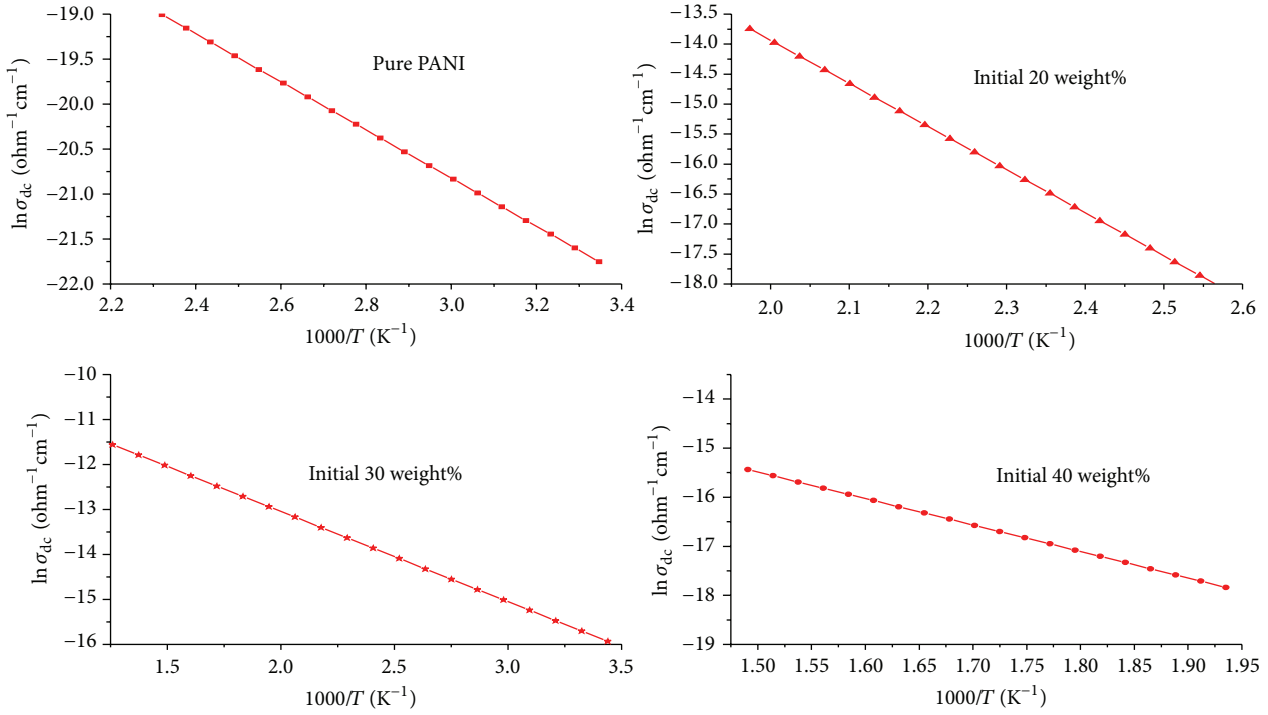

Figure 1: Temperature dependence of DC conductivity in the temperature range (300–550 K) for pure PANI and PANI/V_2O_5 composites (different weight %).

Table 1: Electrical and dielectric parameters of pure PANI and PANI/V_2O_5 composite (different weight %).

Sample	σ_{dc} (Ω^{-1} cm^{-1})	ΔE (eV)	σ_0 (Ω^{-1} cm^{-1})	T = 302 K and f = 850 KHz	
				ε'	ε''
PANI	3.58×10^{-9}	0.22	2.99×10^{-6}	7.59	173.43
PANI/V_2O_5 20 wt%	6.20×10^{-8}	0.61	2.00×10^{-1}	8.35	3158.35
PANI/V_2O_5 30 wt%	2.48×10^{-6}	0.17	1.10×10^{-4}	235.68	3193.48
PANI/V_2O_5 40 wt%	6.16×10^{-8}	0.46	8.6×10^{-4}	242.34	85682.81

3.2. Dielectric Parameters as a Function of Frequency and Temperature. Dielectric parameters as a function of frequency and temperature are calculated using the values of the equivalent parallel capacitance, C_P, dissipation factor, D, and parallel equivalent resistance, R_P, recorded by the LCR meter (Model Wayne Kerr) at selected frequencies range. Temperature dependence of the dielectric constant (ε') and dielectric loss (ε'') is studied for PANI and PANI/V_2O_5 composites in the different range of temperature (300–320 K) and frequency range from 50 kHz to 1 MHz. Dielectric parameters have been calculated using the following equations:

$$\varepsilon' = \frac{C_P}{C_0}, \qquad \varepsilon'' = \frac{\varepsilon'}{\omega C_P R_P} = \varepsilon' D, \tag{2}$$

where $C_0 = (0.08854A/t)$ pf is the geometrical capacitance of vacuum of the same dimensions as that of the sample, A and t are the area and thickness of the sample, respectively, C_P is the capacitance measured in pf, $\omega = 2\pi f$, and $D = \tan\delta$, with δ being the phase angle. The ε' and ε'' are, respectively, the real and imaginary parts of the complex dielectric constant $\varepsilon(f)$, which are represented by the relation

$$\varepsilon(f) = \varepsilon'(f) - i\varepsilon''(f). \tag{3}$$

The dielectric constant of a material consists of ionic, electronic, and dipolar polarizations. Temperature dependence of the dielectric constant (ε') and dielectric loss (ε'') is shown in Figures 2 and 3. It is clear that dielectric constant (ε') and dielectric loss (ε'') remain constant with temperature for pure PANI and 20 weight % of PANI/V_2O_5, whereas a slightly increase is observed in (ε') for 30% and 40% doped samples, and (ε'') slightly increases for 40 weight %. Figures 4 and 5 show variation of dielectric constant and dielectric loss as a function of frequency for pure polyaniline and V_2O_5 composite (different wt%). The results show constant behavior with frequency; their value increases with doping of V_2O_5 (different wt%). At 850 KHz, the dielectric constant for the composite samples with 40 weight % of oxide is about

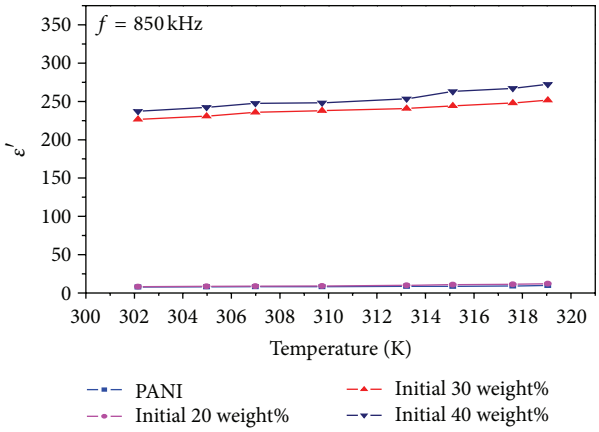

Figure 2: Dielectric constant (ε') versus temperature at fixed frequency for pure polyaniline and PANI/V_2O_5 composites (different weight %).

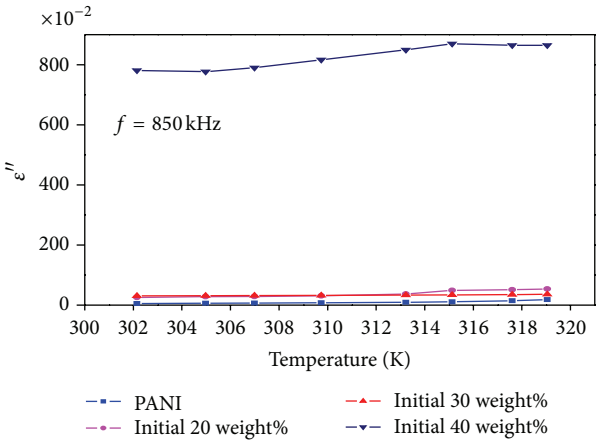

Figure 3: Dielectric loss (ε'') versus temperature at fixed frequency for pure polyaniline and PANI/V_2O_5 composites (different weight %).

242.34. This value decreases to about 8.35 for the composite samples having 20 weight % of oxide. On the other hand, the value of the dielectric constant for pure PANI at this frequency is about 7.59. The corresponding dielectric loss for the composite samples with 40 weight % of oxide is about 85682.81 at 850 KHz frequency. The value decreases to about 3158.35 for the composite with 20 weight % of oxide. Similarly, the value of dielectric loss for pure PANI is about 173.43 at same frequency. Similar trend in the dielectric behaviour of PPy/Fe_3O_4 composites has been reported [33, 34]. Higher dielectric constant and dielectric loss observed with high doping of oxide.

The dielectric loss consists of two contributions, one from the dielectric polarization processes and the other from DC conduction. To study the origin of the dielectric loss in the operating temperature range, the DC conduction loss was calculated using the relation

$$\varepsilon''_{DC} = \frac{\sigma_{DC}}{\varepsilon_0 \omega}. \quad (4)$$

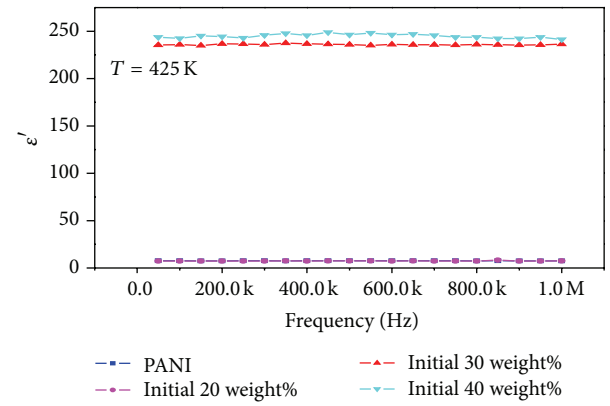

Figure 4: Dielectric constant (ε') versus frequency at fixed temperature (302 K) for pure polyaniline and PANI/V_2O_5 composites (different weight %).

The DC conduction loss is small compared to the observed dielectric loss (ε''). It can also be noted that the DC conduction loss increases with increasing dopant's concentration due to the increase of polarons and bipolarons. Various other workers have also observed such type of behavior [35, 36]. Polaron formation depends upon the viscosity of the medium. The theories based on charged defect centers serve as basis for understanding the dielectric response and conduction mechanisms of such materials. In the correlated barrier hopping model of Elliott (CBH) [37, 38], two electrons are assumed to transfer between charged defect sites (D^+ and D^-) by hopping over a potential barrier separating them. The maximum value of the potential barrier separating the charged defect sites (W_m) can be approximately equated to the band gap of the material. Based on the same model of Elliott [38], the slope obtained from Figure 6 can be written as

$$(m) = \frac{-4kT}{W_m}, \quad (5)$$

where m is defined here as $s - 1$ and m is in line with T. As an outcome of CBH model, the value of s decreases from unity with increasing temperature, and s is a band gap-dependent property [39, 40]. The values of m are calculated from the slopes of these straight lines in Figure 6. The values of m are negative, and the magnitude of m decreases linearly with increasing weight % of V_2O_5. Thus, these results indicate that the observed dielectric dispersion is recognized mainly to dipolar type dispersion in the present study. The DC conduction loss and numerical value of power (m) are given in Table 2.

3.3. Powder X-Ray Diffraction Analysis. XRD patterns of all the four samples, pure PANI, PANI/V_2O_5 composites (with different weight %), show similar structure of amorphous nature in Figure 7. In undoped powder, an intense hump near 19°–24° is found, which is shifted towards lower angle side at 14–18° in doped samples. There are other three small peaks appearing in 20 weight % V_2O_5 doped samples near 15° (200), 20° (001), and at 26° (110), which conform the concentration

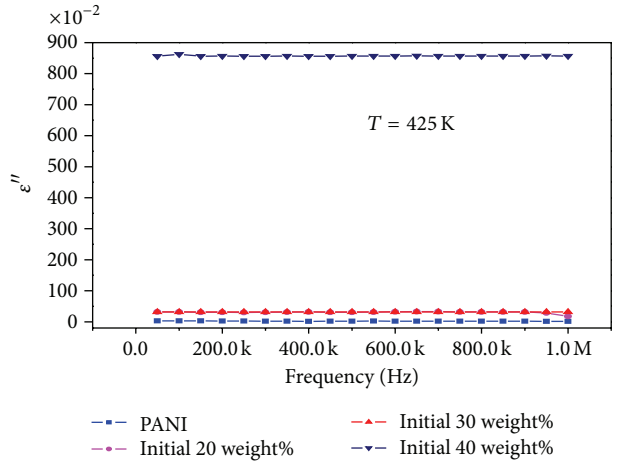

Figure 5: Dielectric loss (ε'') versus frequency at fixed temperature (302 K) for pure PANI and PANI/V_2O_5 composites (different weight %).

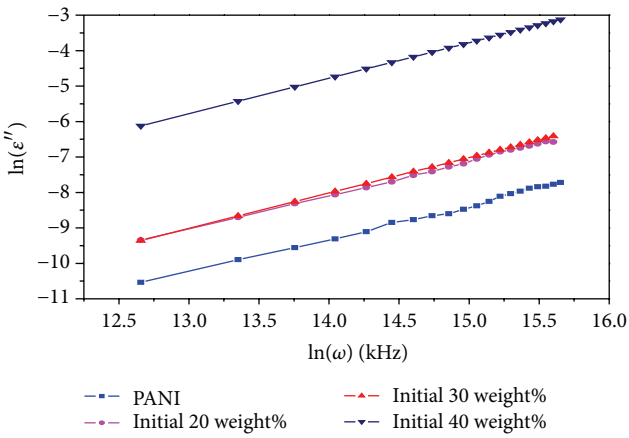

Figure 6: ln(ε'') versus ln(ω) at fixed temperature for pure PANI and PANI/V_2O_5 (different wt%).

Table 2: Temperature dependence of slope (m) and DC conduction loss of pure PANI and PANI/V_2O_5 composites (different weight %).

Sample	ε''_{dc}	(m)	Indirect band gap E_g (eV)
PANI	2.9×10^{-3}	−0.2	3.22
PANI/V_2O_5 20 wt%	1.5×10^{-3}	−0.03	3.27
PANI/V_2O_5 30 wt%	1.28	−0.009	3.31
PANI/V_2O_5 40 wt%	4.8×10^{-3}	−0.0034	3.32

of V_2O_5 in the composites. These peaks continued to be up to 40 weight % doped samples. Thus V_2O_5 dopant is interacting well with PANI; this explains the continuous increase in the conductivity as well as crystallinity of composites. Sharpness of the peaks also shows increase in the crystallinity of composites [41, 42].

3.4. Optical Properties. The optical parameters of the pure PANI and PANI/V_2O_5 composites have been calculated by

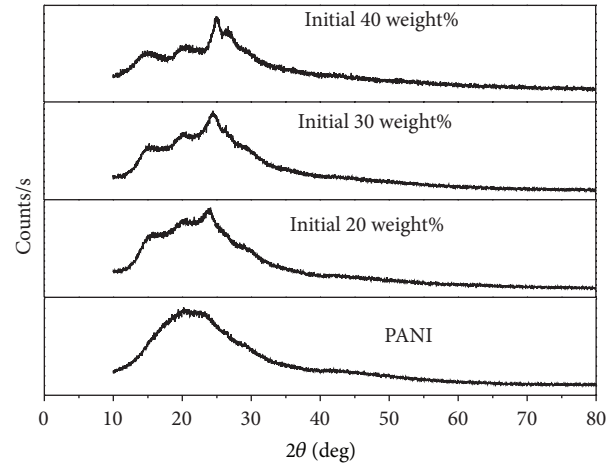

Figure 7: XRD of pure PANI and PANI/V_2O_5 composites (different weight %).

using the UV-spectrophotometer (190–1100 nm). In amorphous materials, the optical band gap between the valence band and the conduction band [43] is given by

$$\alpha h\nu = B\left(h\nu - E_g\right)^m, \tag{6}$$

where "E_g" is the optical band gap and "B" is band tailing parameter related constant. At the fundamental edge of amorphous materials, two types of optical transitions can take place. In both types of optical transitions, the photon interacts with the electron in the valence band and raises it to the conduction band. There is no interaction with lattice in the direct transition, and the photon interacts with lattice in indirect transition. In the given equation "m" decides the transition; for $m = 1/2$ the transition is direct allowed, $m = 2$ for indirect allowed transition, $m = 3$ for indirect forbidden, and $m = 3/2$ for direct forbidden band gap. After applying all values of m, the composites $m = 2$ (indirect transition) is found most suitable to calculate band gap. Extinction coefficient (K) is calculated by using the relation [44]

$$K = \frac{\alpha\lambda}{4\pi}, \tag{7}$$

where "α" is the absorption coefficient and "λ" is the wavelength of photon. The extinction coefficient is a measure of fractional loss due to absorption and scattering per unit distance of the medium participating [45–47]. Figure 8 gives the $(\alpha h\nu)^{1/2}$ dependence on energy for composites. The intercept of slope on x-axis gives the value of optical band gap. The optical band gap measured for pure PANI and PANI/V_2O_5 is given in Table 2 which is found to increase with the increase of the concentration of V_2O_5. Due to the increase in the band gap with V_2O_5 concentration the disorderliness reduces, and defect state density decreases. With the addition of V_2O_5, the unsaturated defects decrease in composites, and a number of saturated bonds are produced. The density of localized states decreases with the reduction in the number of unsaturated defects. According to the Davis and Mott

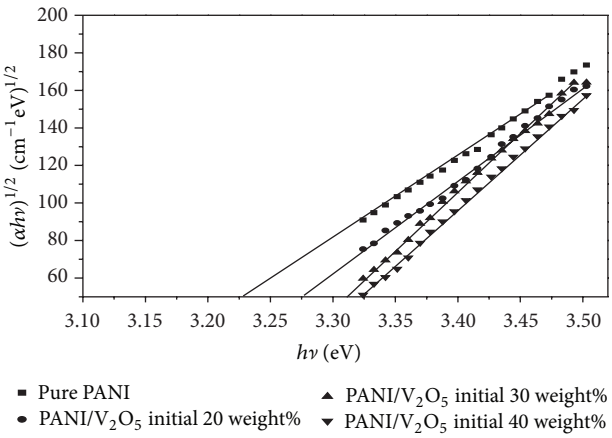

FIGURE 8: $(\alpha h\nu)^{1/2}$ versus photon energy of pure PANI and PANI/V_2O_5 composites (different weight %).

model [48] of density of states, the width of the localized states near the mobility edge depends on defects and degree of disorder present in amorphous structure. It is known that, with saturated bonds, some unsaturated bonds are produced as a result of some insufficient numbers of atoms deposited in the amorphous materials. The high concentration of these localized states is responsible for the low value of optical band gap. The addition of V_2O_5 in the PANI decreases the unsaturated defects producing a number of saturated bonds. This reduction in the unsaturated bonds or defects decreases the density of localized states in band structure increasing the optical band gap.

4. Conclusion

A series of PANI/V_2O_5 composites have been prepared by *in situ* polymerization with different weight percentage of V_2O_5. XRD study reveals the encapsulation of oxide particles by polymer and some degree of crystallinity. The DC conductivity of polyaniline and PANI/V_2O_5 composites together with the dielectric constant and dielectric loss measurements have been determined from the measured values of capacitance in the frequency range from 50 KHz to 1 MHz and in the temperature range of 300–550 K. The conductivity measured is in the range 10^{-7}–10^{-9} S/cm at a temperature 302 K. The conductivity increased with doping, as well as the crystallinity increased when compared to undoped sample. This increase in conductivity of composites at dielectric constant and dielectric loss results indicates that the observed dielectric dispersion is recognized mainly to dipolar type dispersion in the present study and shows independent behavior of frequency. Indirect transition ($m = 2$) is found most suitable to calculate band gap. The optical band gap (E_g) increases as the concentration of V_2O_5 increases; it shows that the disorderliness reduces and defect state density decreases. Dielectric behavior is possible for application in conductive paints, rechargeable batteries, sensors, MOS devices, and so forth.

References

[1] J. Aguilar-Hernández and K. Potje-Kamloth, "Evaluation of the electrical conductivity of polypyrrole polymer composites," *Journal of Physics D: Applied Physics*, vol. 34, no. 11, pp. 1700–1711, 2001.

[2] A. Dey, A. De, and S. K. De, "Electrical transport and dielectric relaxation in Fe_3O_4-polypyrrole hybrid nanocomposites," *Journal of Physics Condensed Matter*, vol. 17, no. 37, pp. 5895–5910, 2005.

[3] C. J. Mathai, S. Saravanan, M. R. Anantharaman, S. Venkitachalam, and S. Jayalekshmi, "Characterization of low dielectric constant polyaniline thin film synthesized by ac plasma polymerization technique," *Journal of Physics D: Applied Physics*, vol. 35, no. 3, pp. 240–245, 2002.

[4] T. K. Vishnuvardhan, V. R. Kulkarni, C. Basavaraja, and S. C. Raghavendra, "Synthesis, characterization and a.c. conductivity of polypyrrole/Y_2O_3 composites," *Bulletin of Materials Science*, vol. 29, no. 1, pp. 77–83, 2006.

[5] W. Chen, L. Xingwei, X. Gi, W. Zhaoquang, and Z. Wenquing, "Magnetic and conducting particles: preparation of polypyrrole layer on Fe_3O_4 nanospheres," *Applied Surface Science*, vol. 218, no. 1–4, pp. 216–222, 2003.

[6] S. D. Patil, S. C. Raghavendra, M. Revansiddappa, P. Narsimha, and M. V. N. A. Prasad, "Synthesis, transport and dielectric properties of polyaniline/Co_3O_4 composites," *Bulletin of Materials Science*, vol. 30, no. 2, pp. 89–92, 2007.

[7] C. Li and G. Shi, "Synthesis and electrochemical applications of the composites of conducting polymers and chemically converted graphene," *Electrochimica Acta*, vol. 56, no. 28, pp. 10737–10747, 2011.

[8] Y. Chen, C. Xu, and Y. Wang, "Viscoelasticity behaviors of lightly cured natural rubber/zinc dimethacrylate composites," *Polymer Composites*, vol. 33, pp. 1206–1214, 2012.

[9] T. Matsunaga, H. Daifuku, T. Nakajima, and T. Gawa-goe, "Development of polyaniline-lithium secondary battery," *Polymers for Advanced Technologies*, vol. 1, no. 1, pp. 33–39, 1990.

[10] G. Gustafsson, Y. Cao, G. M. Treacy, F. Klavetter, N. Colaneri, and A. J. Heeger, "Flexible light-emitting diodes made from soluble conducting polymers," *Nature*, vol. 357, no. 6378, pp. 477–479, 1992.

[11] A. Olcani, M. Abe, M. Ezoe, T. Doi, T. Miyata, and A. Miyake, "Synthesis and properties of high-molecular-weight soluble polyaniline and its application to the 4MB-capacity barium ferrite floppy disk's antistatic coating," *Synthetic Metals*, vol. 57, p. 3969, 1993.

[12] J. Yang, J. Hou, W. Zhu, M. Xu, and M. Wan, "Substituted polyaniline-polypropylene film composites: preparation and properties," *Synthetic Metals*, vol. 80, no. 3, pp. 283–289, 1996.

[13] C. O. Yoon, M. Reghu, D. Moses, Y. Cao, and A. J. Heeger, "Transports in blends of conducting polymers," *Synthetic Metals*, vol. 69, no. 1-3, pp. 255–258, 1995.

[14] R. Murugesan and E. Subramanian, "Charge dynamics in conducting polyaniline-metal oxalate composites," *Bulletin of Materials Science*, vol. 26, no. 6, pp. 529–535, 2003.

[15] C. Brosseau, P. Queffelec, and P. Talbot, "Microwave characterization of filled polymers," *Journal of Applied Physics*, vol. 89, no. 8, article 4532, 2001.

[16] A. G. Mac Diarmid, J. C. Chiang, M. Halpern et al., ""Polyaniline": interconversion of metallic and insulating forms," *Molecular Crystals and Liquid Crystals*, vol. 121, no. 1–4, pp. 173–180, 1985.

[17] S. P. Armes and J. F. Miller, "Optimum reaction conditions for the polymerization of aniline in aqueous solution by ammonium persulphate," *Synthetic Metals*, vol. 22, no. 4, pp. 385–393, 1988.

[18] M. L. Gautu and P. J. G. Romero, "Synthesis and characterization of intercalate phases in the organic-inorganic polyaniline/V_2O_5 system," *Journal of Solid State Chemistry*, vol. 147, no. 2, pp. 601–608, 1999.

[19] W. Jia, E. Segal, D. Kornemandel, Y. Lamhot, M. Narkis, and A. Siegmann, "Polyaniline-DBSA/organophilic clay nanocomposites: synthesis and characterization," *Synthetic Metals*, vol. 128, no. 1, pp. 115–120, 2002.

[20] S. J. Su and N. Kuramoto, "Processable polyaniline-titanium dioxide nanocomposites: effect of titanium dioxide on the conductivity," *Synthetic Metals*, vol. 114, no. 2, pp. 147–153, 2000.

[21] S. Wang, Z. Tan, Y. Li, L. Sun, and T. Zhang, "Synthesis, characterization and thermal analysis of polyaniline/ZrO_2 composites," *Thermochimica Acta*, vol. 441, no. 2, pp. 191–194, 2006.

[22] M. A. M. Khan, M. Zulfequar, A. Kumar, and M. Husain, "Conduction mechanism in amorphous Se75In25-xPb x films," *Materials Chemistry and Physics*, vol. 87, no. 1, pp. 179–183, 2004.

[23] G. T. Kim, J. Muster, V. Krstic et al., "Field-effect transistor made of individual V_2O_5 nanofibers," *Applied Physics Letters*, vol. 76, no. 14, pp. 1875–1877, 2000.

[24] Q. H. Wu, A. Thissen, W. Jaegermann, and M. Liu, "Photoelectron spectroscopy study of oxygen vacancy on vanadium oxides surface," *Applied Surface Science*, vol. 236, no. 1–4, pp. 473–478, 2004.

[25] C. V. Ramana, R. J. Smith, O. M. Hussain, C. C. Chusuei, and C. M. Julien, "Correlation between growth conditions, microstructure, and optical properties in pulsed-laser-deposited V_2O_5 thin films," *Chemistry of Materials*, vol. 17, no. 5, pp. 1213–1219, 2005.

[26] G. B. V. S. Lakshmi, V. Ali, A. M. Siddiqui, P. K. Kulriya, and M. Zulfequar, "Optical studies of SHI Irradiated poly(o-toluidine)-PVC blends," *The European Physical Journal—Applied Physics*, vol. 39, no. 3, pp. 251–255, 2007.

[27] Z. H. Khani, M. M. Malik, M. Zulfequar, and M. Husain, "Electrical conduction mechanism in a-$Se_{80-x}Te_xGa_{20}$ films (0<or=x<or=20)," *Journal of Physics: Condensed Matter*, vol. 7, no. 47, pp. 8979–8991, 1995.

[28] P. M. Grant and I. P. Batra, "Band structure of polyacetylene, (CH)x," *Solid State Communications*, vol. 29, no. 3, pp. 225–229, 1979.

[29] J. Fink and G. Leising, "Momentum-dependent dielectric functions of oriented trans-polyacetylene," *Physical Review B*, vol. 34, no. 8, pp. 5320–5328, 1986.

[30] P. Dutta, S. Biswas, M. Ghosh, S. K. De, and S. Chatterjee, "The dc and ac conductivity of polyaniline-polyvinyl alcohol blends," *Synthetic Metals*, vol. 122, no. 2, pp. 455–461, 2001.

[31] S. De, A. Dey, and S. K. Dea, "Charge transport mechanism of vanadium pentoxide xerogel-polyaniline nanocomposite," *The European Physical Journal*, vol. 46, pp. 355–361, 2005.

[32] A. J. Heeger, S. Kivelson, J. R. Schrieffer, and W.-P. Su, "Solitons in conducting polymers," *Reviews of Modern Physics*, vol. 60, no. 3, pp. 781–850, 1988.

[33] A. Dey, A. De, and S. K. De, "Electrical transport and dielectric relaxation in Fe_3O_4-polypyrrole hybrid nanocomposites," *Journal of Physics Condensed Matter*, vol. 17, no. 37, pp. 5895–5910, 2005.

[34] N. N. Mallikarjuna, S. K. Manohar, P. V. Kulkarni, A. Venkataraman, and T. M. Aminabhavi, "Novel high dielectric constant nanocomposites of polyaniline dispersed with γ-Fe_2O_3 nanoparticles," *Journal of Applied Polymer Science*, vol. 97, no. 5, pp. 1868–1874, 2005.

[35] R. Singh, R. P. Tandon, V. S. Panwar, and S. Chandra, "Low-frequency ac conduction in lightly doped polypyrrole films," *Journal of Applied Physics*, vol. 69, no. 4, pp. 2504–2511, 1991.

[36] N. Musahwar, M. A. Majeed Khan, M. Husain, and M. Zulfequar, "Dielectric and electrical properties of Se-S glassy alloys," *Physica B: Condensed Matter*, vol. 396, no. 1-2, pp. 81–86, 2007.

[37] S. R. Elliott, "A theory of a.c. conduction in chalcogenide glasses," *Philosophical Magazine*, vol. 36, no. 6, pp. 1291–1304, 1977.

[38] S. R. Elliott, "Temperature dependence of a.c. conductivity of chalcogenide glasses," *Philosophical Magazine B*, vol. 37, pp. 553–560, 1978.

[39] J. C. Giuntini, J. V. Zanchetta, D. Jullien, R. Eholie, and P. Houenou, "Temperature dependence of dielectric losses in chalcogenide glasses," *Journal of Non-Crystalline Solids*, vol. 45, no. 1, pp. 57–62, 1981.

[40] W. K. Lee, J. F. Liu, and A. S. Nowick, "Limiting behavior of ac conductivity in ionically conducting crystals and glasses: a new universality," *Physical Review Letters*, vol. 67, no. 12, pp. 1559–1561, 1991.

[41] H. K. Chaudhari and D. S. Kekler, "X-ray diffraction study of doped polyaniline," *Journal of Applied Polymer Science*, vol. 62, no. 1, pp. 15–18, 1996.

[42] B. P. Barbero and L. E. Cadus, "V_2O_5-$SmVO_4$ mechanical mixture: oxidative dehydrogenation of propane," *Applied Catalysis A: General*, vol. 237, no. 1-2, pp. 263–273, 2002.

[43] J. I. Pankove, *Optical processes in Semiconductors*, Prentice-Hall, Englewood Cliffs, NJ, USA, 1971.

[44] A. Abdel-Aal, "Dielectric relaxation in Cd_xInSe_{9-x} chalcogenide thin films," *Egyptian Journal of Solids*, vol. 29, p. 293, 2006.

[45] G. D. Cody, C. R. Wronski, B. Abeles, R. B. Stephens, and B. Brooks, "Optical characterization of amorphous silicon hydride films," *Solar Cells*, vol. 2, no. 3, pp. 227–243, 1980.

[46] J. Tauc, *Amorphous and Liquid Semiconductors*, Plenum Press, NewYork, NY, USA, 1974.

[47] E. Marquez, J. Ramirez-Malo, P. Villares, R. Jimenez-Garay, P. J. S. Ewen, and A. E. Owen, "Calculation of the thickness and optical constants of amorphous arsenic sulphide films from their transmission spectra," *Journal of Physics D: Applied Physics*, vol. 25, no. 3, pp. 535–541, 1992.

[48] N. F. Mott and E. A. Davis, *Electronics Processes in Non-Crystalline Materials*, Clarendon, Oxford, UK, 1979.